Neurofeedback of prefrontal unit activity during working memory in the macaque

Atsushi Noritake[1,2,3], Kazuyuki Samejima[3], Masataka Watanabe[4], Masamichi Sakagami[3]

[1]Division of Behavioral Development, Department of System Neuroscience, National Institute for Physiological Sciences, National Institutes of Natural Sciences.

[2]Department of Physiological Sciences, School of Life Science, The Graduate University for Advanced Studies (SOKENDAI).

[3]Tamagawa University, Brain Science Institute

[4]Tokyo Metropolitan Institute of Medical Sciences

*Correspondence should be addressed to Masamichi Sakagami (sakagami@lab.tamagawa.ac.jp) and Atsushi Noritake (noritake@nips.ac.jp)

Keywords:

Neurofeedback, working memory, lateral prefrontal cortex, non-human primate, single-unit recording

Author contributions:

A.N., M.W., and M.S. designed the experiments. A.N. and M.S. performed the experiments. A.N. and K.S. analyzed the data. All authors contributed to writing the manuscript.

Abstract

Techniques utilizing neurofeedback, a form of biofeedback using neural signals from the brain, have been applied lately to higher association areas such as the lateral prefrontal cortex (LPFC); however, it remains unexplored how well neurofeedback using unit activity in the LPFC modulates its working memory-related activity and performance. To address this issue, we provided neurofeedback of LPFC unit activity during a delay period to two monkeys while they performed a delayed matching-to-paired-sample task. In the task, neurofeedback allowed the animals to shorten the delay length by increasing delay activity and make an earlier choice. Neurofeedback significantly increased delay activity in two-thirds of task-related neurons. Notably, in 16% of these neurons, a preference for delay activity and performance dependent on the stimulus emerged. Although neurofeedback decreased performance primarily due to choice errors, the disassociation of neurofeedback linkage rescued performance. Further, the neuronal activity of simultaneously recorded neurons without neurofeedback linkage suggests that neurofeedback reconfigured the net activity of the LFPC to adapt to new situations. These findings indicate that LPFC neurons can dynamically multiplex different types of information to adapt to environmental changes. Thus, we demonstrated the significant potential of neurofeedback using unit activity to investigate information processing in the brain.

Introduction

Working memory (WM), which is highly developed in primates, maintains relevant information and suppresses irrelevant information over time. WM enables animals to adopt a consistent strategy and behavior to adapt to environmental changes. Previous studies revealed that neuronal activity in the lateral prefrontal cortex (LPFC) is profoundly involved in WM function (Parthasarathy et al., 2017; Rouzitalab et al., 2023; Sakagami and Niki, 1994; Spaak et al., 2017). Electrophysiological analysis in non-human primates has shown that after training in WM tasks, the number of recruited PFC neurons increases during stimulus presentation and a delay period (Qi et al., 2011, 2012). Moreover, the variability of firing rates across trials and correlation discharges, such as noise correlation and across-trial correlation between neurons, decreases (Qi and Constantinidis, 2012a, b). These findings shed light on the PFC neural plasticity and information-coding manner of the PFC in which neurons can tune their activity to adapt to environmental changes through training (Duncan, 2001; Miller and Cohen, 2001). However, studying such learning via training requires devices to track and monitor long-term changes in neural activity, and it remains unclear how such modifications occur.

Feedback techniques using biological signals, termed biofeedback, such as myopotentials (Giggins et al., 2013), electroencephalograms (Gruzelier, 2014), and brain blood oxygen level-dependent signals (Shibata et al., 2011), have a significant potential by quickly making a shortcut link between activity, behavior, and outcome, e.g., reward or punishment. In particular, neurofeedback, a biofeedback technique using neural signals from the brain, has been utilized preferentially to target neural activity in motor-related brain areas (Andersen et al., 2004; Carp et al., 2006; Chapin et al., 1999; Fetz and Baker 1973) including the primary motor area, premotor areas, and frontal eye field. Yet, few studies have examined how neurofeedback modulates activity in higher association areas related to cognitive functions (Cerf et al., 2010; Ishikawa et al., 2014), such as the LPFC (Seitz, 2013; Zhang et al., 2013). A pioneering study demonstrated that visual neurofeedback of single-unit activity in the primate LPFC could increase or decrease its activity in a task-deoebdebt manner (Kobayashi et al., 2010). In that study, the animals could move visual stimuli on a display using LPFC unit activity and attain a liquid reward when the increased or decreased neuronal activity reached some criteria, i.e., neuronal modulation resulted in reward delivery. However, as many LPFC neurons are thought to encode WM-related information (Amemori and Sawaguchi, 2006; Kennerley and Wallis, 2009; Kobayashi et al., 2002; Leon and Shadlen, 1999; Rainer et al., 1999), neurofeedback of their activity could be more directly associated with aspects of WM, rather than reward and its expectation (Lauwereyns et al., 2001; Watanabe et al., 2007). For example, neurofeedback using delay activity, which is not directly associated with outcome, can modify the WM component and subserve WM task performance. In addition, neurofeedback allows us to track unit activity modulation more easily through environmental changes, i.e., before and after neurofeedback, compared with long-term training.

To explore this possibility, we provided neurofeedback of single-unit activity in the LPFC only during a delay period while monkeys performed a delayed matching-to-paired-sample task (DMPST) (Rainer et al., 1999; Sakai and Miyashita, 1991). In this task, the animal was required to choose the paired

associate of a sample stimulus between options after a delay period for a liquid reward. We provided visual feedback of neuronal activity (neurofeedback) in the LPFC during the delay period (**Fig. 1a**) and examined how neurofeedback modified delay activity. We found that neurofeedback allowed the animals to shorten the length of the delay period by increasing firing rates during the delay period and have an earlier chance of making a choice. Conversely, the delay period could be lengthened when neuronal delay activity was decreased. Thus, neurofeedback modification of delay activity did not seem to be linked directly to reward-related components, but rather to WM components.

We hypothesize that neurofeedback motivated the animals to shorten the length of the delay period and improve performance by increasing neuronal activity in the LPFC predominantly during the delay period because previous studies on WM function revealed that monkeys perform better as delay length decreases (e.g., Sakurai, 2001).

Results

Two monkeys were trained to perform the DMPST (see Methods; **Fig. 1b**). In the task, the animal was required to gaze at a fixation point presented at the center of a monitor screen (fixation period) and then to remember a sample stimulus that appeared over the fixation point (sample period). After 0.5-s presentation of the sample stimulus, it disappeared, and a delay period started. During the delay period, two small rectangles moved apart from the center of the screen toward the left and right edges of the screen, respectively. At the end of the delay period, the rectangles reached the horizontal screen edges and disappeared. The animal was required to maintain its gaze at the fixation point during the delay period. After the delay period, it had to choose the paired associate of the sample stimulus between two test stimuli presented peripherally (test period; **Fig. 1b**) by a saccade. A water reward (0.1 mL) was delivered when the animal chose the paired associate correctly (correct trials), whereas no reward was delivered when the animal made the incorrect choice (choice-error trials) or moved their eyes out of a 3° visual window on the fixation point (fixation-break trials). In the experiment, two sample stimuli (S1 and S2) and two test stimuli (T1 and T2) were used; S1 was paired with T1, and S2 was paired with T2 (**Fig. 1c**).

The animals were exposed to at least two trial blocks: control and neurofeedback blocks. In the control blocks, the movement of the rectangles during the delay period was constant and not associated with thedelay activity, while in the neurofeedback blocks, their movement was associated with delay activity and triggered per spike. The fixation point was yellow in the neurofeedback blocks and blue in the control blocks. A pair of the control and neurofeedback blocks was referred to as a session. The control blocks always preceded the neurofeedback blocks to determine the step size of rectangle movement in the following neurofeedback blocks; step size was the value of the mean firing rate during the delay period in

the preceding control blocks divided by the half-screen size in pixels. For example, when the mean firing rate in the control blocks was 20 spikes/s, and the half-screen size was 540 pixels, each step of rectangle movement was 27 pixels/spike. This linkage of neuronal activity to rectangle movement allowed the animals to shorten the delay length by increasing the firing rate during the delay period and obtain an earlier opportunity to make a choice, i.e., the more the neuron fired during the delay period, the quicker the rectangles moved toward the screen edges (**Fig. 1b,d**). Such shortening of the delay period benefited the animals because WM load, i.e., maintaining the relevant information over the delay period, was reduced in the neurofeedback blocks compared to the control blocks. Conversely, the delay period would be lengthened when neuronal activity did not reach the criteria (**Fig. 1b,d**). Accordingly, delay length varied across trials in the neurofeedback blocks.

Behavioral data during the DMPST

In 125 sessions of the DMPST, neither monkey exhibited a significantly different performance rate between the stimuli during the neurofeedback blocks (monkey M, 37 recording sessions: 74.7% for stimulus A and 72.3% for stimulus B, $p = 5.2 \times 10^{-1}$, $Z = 0.6$, Mann-Whitney *U*-test; monkey S, 88 recording sessions: 80.5% for stimulus A and 77.7% for stimulus B, $p = 1.2 \times 10^{-1}$, $Z = 1.6$, Mann-Whitney *U*-test) as well as in the control blocks (monkey M: 86.3% for stimulus A and 89.0% for stimulus B, $p = 4.4 \times 10^{-2}$, $Z = 0.8$, Mann-Whitney *U*-test; monkey S: 90.0% for stimulus A and 87.5% for stimulus B, $p = 6.2 \times 10^{-2}$, $Z = 1.9$, Mann-Whitney *U*-test), at the population level. We then merged the stimulus data in some of the following analyses of behavior.

Against our prediction, correct performance was significantly lower in the neurofeedback blocks than in the control blocks for both animals (monkey M: 87.4% in the control blocks vs. 73.3% in the neurofeedback blocks, $p = 3.3 \times 10^{-7}$, $Z = 5.1$; monkey S: 88.4% in the control blocks vs. 80.4% in the neurofeedback blocks, $p = 5.7 \times 10^{-5}$, $Z = 4.0$, Mann-Whitney *U*-test; **Fig. 2a**), although the animals shortened the delay length (**Fig. 2b**) for most of the neurons with neurofeedback (median: 235 ms, $p = 5.6 \times 10^{-7}$, $Z = 5.0$, Mann-Whitney *U*-test). This decrease in performance was primarily due to the increase of delay-length deviation in the neurofeedback blocks from the constant delay length in the control blocks (delay-length modulation), particularly in the excessively modulated epochs (<-600 ms and >600 ms). The delay-length variance among trials in the neurofeedback blocks was also correlated with the decrease in performance (stimulus A: $r = -0.25$, $p = 5.5 \times 10^{-3}$; stimulus B: $r = -0.37$, $p = 2.5 \times 10^{-5}$, Pearson's correlation test; **Fig. 2c**). This would lead to a decay of WM, resulting in an increase in the choice-error rate by choosing the wrong target in both monkeys (monkey M: $p = 4.4 \times 10^{-10}$, $Z = 6.2$, monkey S: $p = 3.2 \times 10^{-13}$, $Z = 7.3$, Mann-Whitney *U*-test; **Fig. 2d**). To verify whether the larger deviation of delay length induced

more choice errors, we plotted the mean choice-error rate as a function of delay-length modulation, which was calculated by subtracting the delay length in the neurofeedback blocks from that in the preceding control blocks (**Fig. 2e**). The choice-error rate was < 10% when the modulation of delay length was moderate (moderate delay-length modulation: -600–0 ms), while it gradually increased for the other delay-length modulations. These results indicate an inverted U-shape function in the correct performance rate against delay-length modulation during the neurofeedback blocks ($p = 2.0\times10^{-10}$, $F_{[2,\ 122]} = 26.9$, quadratic regression test). Particularly, when delay length became short, the animal's decision during neurofeedback might become reactive and immature due to the sudden termination of the delay period, introducing reactive responses (i.e., short saccadic latency) and choice errors. However, saccade latency at choice errors in such a situation (delay-length modulation: <-600 ms), as an index of reactive and immature decision-making, was similar (mean: 215.3 ms) to that in the correct trials under neurofeedback (mean: 218.9 ms; $p = 1.9 \times 10^{-1}$, $t_{211} = 1.3$, Weltch's *t*-test) as well as in the choice-error trials in the control blocks (mean: 211.9 ms; $p = 3.2 \times 10^{-1}$, $t_{356} = 1.0$, Weltch's *t*-test). In contrast, when delay length became long, saccade latency was significantly longer than that in the choice-error trials in the control blocks (mean saccadic latency: 222.4 ms in the control blocks and 226.2 ms in the neurofeedback blocks; $p = 1.2 \times 10^{-2}$, $t_{178} = 2.5$, Weltch's *t*-test) or in the correct trials in the neurofeedback blocks (mean: 211.9 ms; $p = 4.2 \times 10^{-5}$, $t_{303} = 2.5$, Weltch's *t*-test). Thus, choice errors were induced without reactive and immature responses in extensively short delay periods and with more extended saccadic responses in extensively long delay periods.

Neuronal modulation by neurofeedback

Neuronal activity was significantly modulated in the 125 sessions among the fixation, sample, delay, and test periods in the control blocks (task-related neurons, see Methods). A simple comparison of the mean firing rate during the delay period in the neurofeedback blocks to that in the control blocks showed that most task-related neurons (101/125) increased their firing rate during the delay period in a task-dependent manner (increased type); conversely, the remaining neurons decreased their firing rate (24/125, decreased type). These results indicate that a large number of neurons in the LPFC could be modified predominantly during the delay period, albeit with a small modulation before and during the sample period, by neurofeedback in a task-dependent manner (**Fig. S1**). We further inspected this increased activity in the following analyses.

Three types of LPFC neuronal activity during neurofeedback

To examine the impact of neurofeedback on LPFC unit activity, we applied two-way analysis of variance

(ANOVA) with neurofeedback (with or without neurofeedback) and stimulus (S1 or S2) as factors to the firing rate during the delay period for each neuron. As a result, 82 of the 101 increased-type neurons were classified into three neuronal types: Type I, II, and III. Type I neurons showed a significant effect of neurofeedback only (neurofeedback, $p < 0.05$; stimulus, not significant [*n.s.*]; interaction between the neurofeedback and stimulus factors, *n.s*; **Fig. 3a, *top***). Type II neurons exhibited significant neurofeedback and stimulus effects (neurofeedback, $p < 0.05$; stimulus, $p < 0.05$; interaction, *n.s.*; **Fig. 3a, *middle***). Type III neurons exhibited a significant interaction ($p < 0.05$; **Fig. 3a, *bottom***), irrespective of the main factor effects.

Approximately two-thirds of the neurons (54/82, 65.9%) were Type I (example, **Fig. 3b, *top***; population, **Fig. 3b, *bottom***); these neurons increased their activity predominantly in the delay period, irrespective of the sample stimulus, during the neurofeedback blocks compared to the control blocks. Fifteen neurons (18.3%) were Type II (example, **Fig. 3c, *top***; population, **Fig. 3c, *bottom***); these neurons had significantly increased delay activity and preserved the differences between the sample stimuli during neurofeedback. The sample stimulus that induced more delay activity in the neurofeedback blocks was referred to as the "preferred" stimulus and the other as the "non-preferred" stimulus. A relatively small number of neurons were Type III (13/82, 15.8%; example, **Fig. 3d, *top***; population, **Fig. 3d, *bottom***); these neurons exhibited similar delay activity between the sample stimuli during the control blocks. However, in the neurofeedback blocks, a significant difference in delay activity emerged between the sample stimuli. The sample stimulus that induced more delay activity in the neurofeedback blocks was also referred to as the "preferred" stimulus and the other as the "non-preferred" stimulus.

Performance during neurofeedback

We next assessed how the delay activity of each neuronal type was correlated with the correct performance rate depending on the delay-length modulation during the neurofeedback blocks. For this analysis, the correct choice rate was computed separately for Type II and III neurons in two analysis epochs (<-600 ms and -600–0 ms), but the data for both stimuli were merged for Type I neurons because there was no significant difference in all epochs. The correct choice rate of the preferred stimulus for Type III neurons was significantly higher than that of the non-preferred stimulus ($p = 3.5 \times 10^{-2}$, $t_9 = 2.5$, paired *t*-test) and that of Type I neurons ($p = 9.2 \times 10^{-6}$, $t_{55} = 4.9$, Welch's *t*-test) when delay-length modulation was within -600–0 ms (**Fig. 4a**). In contrast, the correct rates were similarly reduced when delay-length modulation was not in this range (< -600 ms). These results suggest that Type III neurons contributed to the high-performance rate for a specific stimulus under neurofeedback in the moderate range of delay-length modulation (-600–0 ms).

Trial-by-trial changes in neuronal delay activity

We further analyzed the trial-by-trial changes in the delay activity of each neuronal type during neurofeedback. For this analysis, we used the neurons for which more than 15 trials of each stimulus were tested during the neurofeedback blocks (Type I: n = 51; Type II: n = 15; Type III: n = 12). All neuronal types increased their delay activity from the first trial for both sample stimuli (**Fig. 4b–d**). These delay-length modifications of Type I and II neurons mostly continued throughout the trials (**Fig. 4c**). Notably, for Type III neurons, the differences between the stimuli in delay activity increased as the trial proceeded, which was formed by a decrease of delay activity for the non-preferred stimulus at the population level (stimulus factor: $p = 9.3 \times 10^{-3}$, $F_{[1, 280]} = 1.79$; interaction: $p = 6.6 \times 10^{-2}$, $F_{[14, 280]} = 1.65$, repeated two-way ANOVA with the trial and stimulus factors; **Fig. 4d**). To determine when the differentiation between the preferred and non-preferred stimuli started, we compared delay activity between the stimuli in each trial during the neurofeedback blocks. The differential activity began on the eighth trial after neurofeedback started ($p < 0.05$; t-test in each trial; **Fig. 4d**). Among the 12 Type III neurons tested, two-thirds (8/12) did not show differential delay activity between the stimuli in the control blocks (*n.s.*, paired t-tests). These results indicate that Type III neurons developed a preference for a specific stimulus throughout neurofeedback.

Modulation of simultaneously recorded neurons without neurofeedback effect

To answer determine whether our neurofeedback method using single-unit activity affected recorded activity specifically or the net activity of neurons in the LPFC, we assessed another 46 simultaneously recorded neurons without neurofeedback linkage ("irrelevant" neurons) and obtained 26 Type I neurons, 7 Type II neurons, and 13 Type III neurons (**Fig. 5**). This finding indicates that similar proportions of Type I and II neurons without neurofeedback linkage to those of Type I and II neurons with neurofeedback linkage were recruited in the net activity of the LPFC. Compared with Type III neurons with neurofeedback, more Type III neurons without neurofeedback linkage would work in the background during the neurofeedback blocks. These findings suggest that neurofeedback influenced the LPFC net activity and strengthened our hypothesis that Type III neurons contributed to the maintenance of correct performance.

Performance in yoked blocks

To test further the effect of neurofeedback linkage on delay activity and length, we provided another control block ("yoked" block) after the neurofeedback blocks in 95 of 125 sessions (15 sessions for monkey M and 80 sessions for monkey S). In the yoked blocks, the association between delay activity and length was

dissected under the control of delay-length variance among trials by replaying the same sequence of delay lengths experienced in the preceding neurofeedback blocks. In contrast to the variable step timing of rectangle movement during the neurofeedback blocks, the rectangles moved at a constant speed in the yoked blocks. The performance in the yoked blocks recovered to a similar level as that in the control blocks (88.5% in the control blocks; 79.2% in the neurofeedback blocks; 88.8% in the yoked blocks; **Fig. 6a**), confirmed by one-way ANOVA ($p = 2.3 \times 10^{-12}$, $F_{[3, 282]} = 29.5$) with the Tukey-Kramer test as a post-hoc test ($p = 1.8 \times 10^{-10}$ between the control and neurofeedback blocks, $p = 4.0 \times 10^{-11}$ between the neurofeedback and yoked blocks; $p = 0.97$ between the control and yoked blocks). This performance recovery was primarily due to the decrease of the choice error proportion relative to that in the neurofeedback blocks (yoked blocks vs. neurofeedback blocks: 4.4% vs. 8.6%, respectively, $p = 7.9 \times 10^{-16}$, $t_{139} = 9.1$, paired *t*-test). To evaluate performance in the yoked blocks further, we plotted the correct performance in each session as a function of delay-length modulation (**Fig. 6b**). Regression analysis revealed that performance was fitted in a linear, but not quadratic, manner ($p = 6.6 \times 10^{-3}$, $r = -2.8 \times 10^{-2}$, Pearson's correlation test). Moreover, performance was not significantly influenced by the variance of delay-length modulation among the trials for each stimulus (stimulus A: $p = 7.7 \times 10^{-2}$, $r = 1.8 \times 10^{-1}$; stimulus B: $p = 3.4 \times 10^{-1}$, $r = 9.9 \times 10^{-2}$, Pearson's correlation test; **Fig. 6c**). Thus, the recovery of performance in the yoked blocks indicated that the delay-length variance among the trials in the neurofeedback blocks was not primarily due to a decrease of performance in the neurofeedback blocks. Instead, neurofeedback likely perturbated net activity, decreasing the correct performance rate.

Discussion

Few neurofeedback studies using the unit activity of LPFC neurons have been reported (Kobayashi et al., 2010; Widge et al., 2018); however, the consequences of neurofeedback were directly linked with rewards in these studies. In the present study, we devised a new task in which the delay period could be shortened by increasing the delay activity of single LPFC neurons, which was not linked directly to outcome. Therefore, our neurofeedback was likely associated with WM rather than reward-related functions. Using this neurofeedback task, we successfully conditioned the delay activity of LPFC neurons and tracked the changes of neuronal activity among the blocks. We identified generally increased neuronal types (Type I, 54/82; Type II, 15/82) and a specific stimulus-preferring neuronal type (Type III, 13/82) in which stimulus preference emerged during neurofeedback without a decrease in performance. Our identification of irrelevant neurons suggests that neurofeedback recruited all types of neurons in the LPFC and reconfigured net activity, such as the proportion of Type I–III neurons and the decreased type neurons or their activity balance, to adapt to situational changes. Thus, we demonstrated that neurofeedback using LPFC unit

activity effectively modified the activity of LPFC neurons to adapt to a new situation.

Despite there being no necessity to shorten the delay length in the neurofeedback blocks, both monkeys did so by effectively increasing the delay activity of most neurofeedback-given neurons (**Figs. 3 and 4**). This indicates that the monkeys were strongly motivated to shorten the delay length, as a large body of work suggests that organisms prefer earlier consequences and deterministic situations rather than delayed, uncertain, or ambiguous situations (Hayden, 2016; Kim et al., 2009; Sakurai, 2001). However, such motivation did not simply contribute to correct performance in our neurofeedback WM task. Excessive increased neuronal modulation induced more choice errors and decreased WM performance (**Fig. 1b,e**). In contrast, decreased neuronal modulation functioned oppositely to lengthen the delay period against the animals' motivation and intention (**Fig. S1**). The decrease in performance was recovered in the yoked blocks despite having the same delay-length variance as in the neurofeedback blocks. This finding also suggests that neurofeedback, not delay-length variance, was involved in the decreased performance and reconfiguration of neuronal activity in the LPFC.

Under neurofeedback, Type I–III neurons conceivably played different roles. Type I neurons may largely reflect the arousal level. Indeed, these neurons increased their activity not only during the delay period but also in the fixation and sample periods in the neurofeedback blocks (**Fig. 3b,c**). Although the enhanced activity predominantly during the delay period might facilitate the processing function of WM, its excessive modulation likely lowered the signal-to-noise ratio of relevant information to irrelevant information and would decrease the performance rate. Some electrophysiological studies using non-human primates support this notion (Qi et al., 2011, 2012) by demonstrating that more PFC neurons are recruited during stimulus presentation and delay period in WM tasks, but the mean selectivity of individual neurons to discriminate stimuli decreases. These findings suggest that balancing the recruited neuron population and representation activity of relevant information would be crucial to optimize the signal-to-noise ratio for WM. Type II neurons may robustly contribute to the correct choice by maintaining differential delay activity throughout the situation changes. Type III neurons could also contribute to correct performance in the neurofeedback and yoked blocks after preference activity has developed. The emergence of preference may reflect adaptation to the situational changes during the neurofeedback blocks.

This view is consistent with the framework of adaptive coding to environments, which contains concepts of WM and selective attention and control (Duncan, 2001; Gdalyahu et al., 2012; Watanabe and Sakagami, 2007). It hypothesizes that PFC neurons simultaneously encode different types of information, i.e., multiplex, related to current concerns and behavior, such as stimuli, responses, memory, and reward, by inactivating and activating neurons in a situation-dependent manner. The decreased type neurons, albeit representing a small population in the LPFC, might play a critical role in regulating the activity of LPFC

neurons, even against the task demand and the animal's will. Our identification of these neuronal types may be proof of adaptive coding in the LPFC.

The emergence of preference in WM function, as observed for the activity of Type III neurons (**Fig. 4d**), is often described by recurrent neural network models using excitatory and inhibitory units. Such models can successfully trace the delay activity of PFC neurons and generate a preference or tuning to a specific stimulus through training in WM tasks (Liu et al., 2021; Wang, 2002, 2008). Indeed, cortical circuits, including the LPFC, have recurrent connections (Camperi and Wang, 1998; Goldman-Rakic, 1995). Despite having a different time scale from the models in these studies, our findings of the emergence of preference in Type III neurons and increase and decrease neuronal types, i.e., Type I and II neurons, were consistent with their results. The use of recurrent neural network models may also subserve to study the relationships between behaviors and unit activity, mainly to understand the neuronal characteristics of Type III neurons, decrease type neurons, and the excitation-inhibition balance in future studies.

On the basis of the neuronal modulation induced by neurofeedback, net reconfiguration conceivably occurred not only in the LPFC but also in other brain regions such as the ventral striatum (Pereira et al., 2023), parietal cortices (Garrison et al., 2021), and medio-fronto cortices including the dorsolateral PFC, premotor area, and supplemental motor area (Newton et al., 2011) during WM tasks. In fact, the reorganization of these networks has been observed under neurofeedback training in a WM task, although this training was provided solely to dorsolateral PFC activity (Zhang et al., 2015). That study also reported increases and decreases of activity in the targeted brain region through training and neurofeedback, similarly to our case. These studies and our findings also suggest that the balance of excitation and inhibition in these brain networks including the LPFC may play a critical role in maintaining or increasing WM performance.

The observed decrease in correct performance is consistent with the results of the previous studies showing that performing dual tasks interferes with the performance of each task (Watanabe and Funahashi, 2018). In such dual tasks, the ability of prefrontal neurons to represent task-relevant information decreases as the demand for the concurrent counterpart task increases (Watanabe and Funahashi, 2014). These studies suggest that the decrease in performance in our task could be due to the overload of multitasking cognitive control by neurofeedback (Cole et al., 2013; Cole et al., 2012). In multitasking cognitive control situations, the same LPFC neural population are simultaneously recruited and overloaded by the multiple tasks. Consequently, the limited neural resources in the LPFC are shared, which impairs the performance of the targeted task. In our case, during the delay period in the neurofeedback blocks, the monkeys might face dual cognitive operations, i.e., retaining the sample stimulus in WM and shortening the delay period by increasing the delay activity. The increased activity of Type I–III neurons might reduce the neural resources

available for WM and decrease performance. In contrast, in the yoked blocks, in which the association between delay activity and length was dissected, the resource of delay activity was released, and the performance recovered. Thus, our findings might demonstrate that LPFC neurons adapted to the new neurofeedback situation under multitasking with the constraint of finite resources. Another possibility is insufficient adaptation time for the animals. Previous work that successfully improved the performance of WM tasks included a training period using neurofeedback for adaptation to the neurofeedback condition, whereas we provided neurofeedback immediately after the control block. Such a manner of applying neurofeedback might not supply the animals with sufficient time for a better or optimal reorganization of the local network in the LPFC or the WM-related network, resulting in the increase of choice errors and similar saccadic latency at choice errors with short delay-length modulation in the neurofeedback blocks compared to those in the control blocks.

In this study, we used neurofeedback of single-unit activity. However, it is possible that neurofeedback of net LPFC activity can manipulate and improve WM performance more precisely, as observed in imaging studies using neurofeedback approaches with various computational algorithms, e.g., decoded neurofeedback [DecNef] and real-time functional magnetic resonance image techniques, in which brain activity is led to a target state to improve the learning of subthreshold perception (Shibata et al., 2011) and motor-related dysexecutive behavior clinically (Mazrooyisebdani et al., 2018; Mohanty et al., 2018; Papoutsi et al., 2018). A further step is to directly and causally manipulate the net state of LPFC neuronal activity in WM tasks and identify how these three neuronal types and the decreased type contribute to WM performance.

Methods

General

All experimental surgical protocols were approved by the Animal Care and Use Committee at Tamagawa University and were in accordance with the US National Institutes of Health Guide for the Care and Use of LaboratoryAnimals. Two male Japanese monkeys (*Macaca fuscata*, monkey M: 6.5 kg and monkey S: 7.0 kg) were the subjects in the present study. Each animal was mildly fluid deprived during the task-training and experimental periods. In the experiment, the monkey sat in a primate chair inside a sound-attenuated room with its head fixed. Visual stimuli were presented on a 21-inch computer monitor (FlexScan T966, EIZO, Ishikawa, Japan) placed 90.0 cm in front of the monkey at eye level. We recorded single-unit activity around the principal sulcus area in the left hemispheres by using a tungsten electrode (diameter, 0.25 mm; 0.5–2 MΩ; Frederick Haer, Bowdoinham, ME, USA). The recording sites were determined by reference to magnetic resonance images (**Fig. 1a**). Eye position was monitored at 240 Hz

by an infrared eye-tracking system (resolution, 0.25° in visual angle; EYE-TRAC6; Applied Science Laboratories, Bedford, MA, USA). The Tempo system (Reflective Computing, Olympia, WA, USA) was used to control the experiment and data acquisition with 1-ms temporal resolution.

Surgical procedures

Under sterile conditions, the monkeys were surgically prepared under ketamine HCl (10 mg/kg, i.m.) and pentobarbital-induced anesthesia (Nembutal, 25 mg/kg, i.p.; note that this study was conducted during the lawful allowance of pentobarbital-induced anesthesia.) After exposing the skull, acrylic screws were installed to fasten dental acrylic head implants to the skull. A hollow rod (diameter, 15 mm) was attached to the skull with dental acrylic for head fixation. A recording chamber (30 × 40 mm) was positioned stereotaxically over the LPFC (left hemisphere in both animals) to access the ventral and dorsal areas around the principal sulcus (**Fig. 1a**) and secured with dental acrylic. Antibiotics (ampicillin, i.m., total 1 g/day) and analgesics (diclofenac sodium, 6.25 mg) were administered on the day of surgery and for seven and three days postoperatively, respectively. Craniotomy was performed after the monkeys had learned the control tasks well (performance > 85%).

DMPST

We trained the animals to perform a visual DMPST. A trial started with the presentation of a fixation point at the center of the monitor screen (**Fig. 1b**). The animal was required to fixate on it for at least 700 ms (fixation period) within a diameter of 3°. A sample stimulus was then presented for 500 ms at the center of the screen (sample period), followed by a delay (delay period). At the beginning of the delay period, the fixation color changed to red, and two small rectangles appeared at 3° below the stimulus. Each rectangle moved horizontally, away from the other, toward the right and left edges of the screen at the same speed. When both rectangles reached the edges, they disappeared, indicating the end of the delay period. Two test stimuli then appeared at 5° right and left from the screen center. The animal was required to choose one of them by making a saccadic eye movement in 500 ms and hold it for at least 300 ms within a 3° diameter. A water reward (0.1 mL per trial) was delivered when the animal chose the paired associate correctly (correct trials). In the experiment, two sample stimuli (S1 and S2) and two test stimuli (T1 and T2) were used; S1 was paired with T1, and S2 was paired with T2 (**Fig. 1c**). One of the sample stimuli was used pseudorandomly in a trial. The right-left positions of the test stimuli were also determined pseudorandomly.

No reward was delivered when the animal made eye-fixation breaks, eye position outside of a 3° visual window (fixation-break error trials), or wrong choices by choosing the unpaired target (choice-error trials). Since eye fixation was required during the fixation, sample, and delay periods, breaking fixation

during these periods resulted in trial termination with a time-out period of 5 s in addition to the inter-trial interval (3–4 s). After a fixation-break error, the same stimulus and test stimuli were presented in the subsequent trial (correction trials). In the correction trials, half the reward (0.05 mL) was delivered when the animal correctly chose the paired associate. The correction trials were excluded from the analysis.

Control, neurofeedback, and yoked block

The animals were exposed to at least control and neurofeedback blocks. In the control blocks, the movement of the rectangles during the delay period was not associated with delay activity; the rectangles moved at a constant speed and reached the screen edges at the end of the delay period. The control blocks always preceded the neurofeedback blocks to determine the speed of rectangle movement. In the neurofeedback blocks, rectangle movement was associated with the delay activity of the recorded neurons, i.e., the spike firing rate during the delay period drove the movement of the rectangles. The step size of rectangle movement per spike was determined as a value of the mean firing rate during the delay period in the preceding control blocks divided by the half-screen size in pixels. When the value was indivisible, it was rounded down to the nearest decimal. When the firing pulses of the recorded neurons reached the spike number of the mean firing rate measured in the control blocks, the rectangles reached the screen edges. This linkage of neuronal activity with rectangle movement allowed the animals to shorten the delay length by increasing the firing rate during the delay period and obtain an earlier opportunity of target choice. The more the recording neuron fired during the delay period, the quicker the rectangles moved toward the screen edges (**Fig. 1b,d**). Conversely, the delay period would be lengthened when the recorded neuron fired less than in the control blocks (**Fig. 1b,d**). Consequently, delay length could vary across trials in the neurofeedback blocks. A pair of the control and neurofeedback blocks was referred to as a session. A single session was tested for each neuron, i.e., one control and one neurofeedback blocks were tested for each neuron. In 95 of 125 sessions, a yoked block was additionally provided for the animals (15 sessions for monkey M and 80 sessions for monkey S). In the yoked blocks, the same sequence of delay lengths and stimuli experienced in the preceding neurofeedback blocks was replayed, but with constant rectangle movement speed. Thus, the rectangles moved at a constant speed during the delay period in the control and yoked conditions. but not in the neurofeedback blocks. A trial was terminated when delay length was >5 s due to the lower activity of the targeted neurons in the neurofeedback blocks than in the control blocks. Delay length in the control blocks was constant in a block and varied among the sessions (median length, 1,400 ms; interquartile range, 200 ms) to weaken the temporal prediction of delay length. The color of the fixation point instructed the animal as to which block it was to perform: blue for the control blocks, yellow for the neurofeedback blocks, and green for the yoked blocks.

Measurement of eye position and movement

To examine the relationships between neuronal activity and eye movement, we measured the horizontal and vertical eye positions and smoothed them using a Gaussian kernel (σ = 10 ms, width = 3 σ). We calculated the onset, offset, peak velocity, amplitude, and duration of saccadic eye movement using the vector data of the square root ($dx^2 + dy^2$) of eye position at a time resolution of 1 ms. Saccade onset was defined as the first time when the angular velocity of a saccade exceeded 30°/s. Saccade offset was defined as the first time when the angular velocity of a saccade was less than 30°/s after saccade onset. The period and maximum velocity between saccade onset and offset were used as saccade duration and peak velocity, respectively. Saccadic amplitude was defined as the distance in degrees between the saccade onset and offset points.

Task-related neurons

A neuron was classified as a task-related neuron when it showed a significant difference in its firing rate by repeated ANOVA ($p < 0.05$) during at least one of the five epochs in the control blocks: pre-sample cue epoch (0.5 s before sample cue onset), post-sample cue epoch (0.5 s after sample cue onset), delay epoch (0.5–1.0 s after sample cue onset), pre-test stimulus epoch (0.5 s before test stimulus), and post-test stimulus epoch (0.5 s after the test stimuli). In all 125 sessions, we used the neurons that exhibited significant modulation in the control blocks of the task (task-related neurons) for our neurofeedback study.

References

Amemori, K., Sawaguchi, T., 2006. Contrasting effects of reward expectation on sensory and motor memories in primate prefrontal neurons. Cereb Cortex 16, 1002-1015.

Andersen, R.A., Musallam, S., Pesaran, B., 2004. Selecting the signals for a brain-machine interface. Curr Opin Neurobiol 14, 720-726.

Camperi, M., Wang, X.J., 1998. A model of visuospatial working memory in prefrontal cortex: recurrent network and cellular bistability. J Comput Neurosci 5, 383-405.

Carp, J.S., Tennissen, A.M., Chen, X.Y., Wolpaw, J.R., 2006. H-reflex operant conditioning in mice. J Neurophysiol 96, 1718-1727.

Cerf, M., Thiruvengadam, N., Mormann, F., Kraskov, A., Quiroga, R.Q., Koch, C., Fried, I., 2010. On-line, voluntary control of human temporal lobe neurons. Nature 467, 1104-1108.

Chapin, J.K., Moxon, K.A., Markowitz, R.S., Nicolelis, M.A., 1999. Real-time control of a robot arm using simultaneously recorded neurons in the motor cortex. Nat Neurosci 2, 664-670.

Cole, D.M., Oei, N.Y., Soeter, R.P., Both, S., van Gerven, J.M., Rombouts, S.A., Beckmann, C.F., 2013. Dopamine-dependent architecture of cortico-subcortical network connectivity. Cereb Cortex 23, 1509-1516.

Cole, M.W., Yarkoni, T., Repovs, G., Anticevic, A., Braver, T.S., 2012. Global connectivity of prefrontal cortex predicts cognitive control and intelligence. J Neurosci 32, 8988-8999.

Duncan, J., 2001. An adaptive coding model of neural function in prefrontal cortex. Nat Rev Neurosci 2, 820-829.

Fetz, E.E., Baker, M.A., 1973. Operantly conditioned patterns on precentral unit activity and correlated responses in adjacent cells and contralateral muscles. J Neurophysiol 36, 179-204.

Garrison, J.R., Saviola, F., Morgenroth, E., Barker, H., Luhrs, M., Simons, J.S., Fernyhough, C., Allen, P., 2021. Modulating medial prefrontal cortex activity using real-time fMRI neurofeedback: Effects on reality monitoring performance and associated functional connectivity. Neuroimage 245, 118640.

Gdalyahu, A., Tring, E., Polack, P.O., Gruver, R., Golshani, P., Fanselow, M.S., Silva, A.J., Trachtenberg, J.T., 2012. Associative fear learning enhances sparse network coding in primary sensory cortex. Neuron 75, 121-132.

Giggins, O.M., Persson, U.M., Caulfield, B., 2013. Biofeedback in rehabilitation. J Neuroeng Rehabil 10, 60.

Goldman-Rakic, P.S., 1995. Cellular basis of working memory. Neuron 14, 477-485.

Gruzelier, J.H., 2014. EEG-neurofeedback for optimising performance. III: a review of methodological and theoretical considerations. Neurosci Biobehav Rev 44, 159-182.

Hayden, B.Y., 2016. Time discounting and time preference in animals: A critical review. Psychon Bull Rev 23, 39-53.

Ishikawa, D., Matsumoto, N., Sakaguchi, T., Matsuki, N., Ikegaya, Y., 2014. Operant conditioning of synaptic and spiking activity patterns in single hippocampal neurons. J Neurosci 34, 5044-5053.

Kennerley, S.W., Wallis, J.D., 2009. Reward-dependent modulation of working memory in lateral prefrontal cortex. J Neurosci 29, 3259-3270.

Kim, S., Hwang, J., Seo, H., Lee, D., 2009. Valuation of uncertain and delayed rewards in primate prefrontal cortex. Neural Netw 22, 294-304.

Kobayashi, S., Lauwereyns, J., Koizumi, M., Sakagami, M., Hikosaka, O., 2002. Influence of reward expectation

on visuospatial processing in macaque lateral prefrontal cortex. J Neurophysiol 87, 1488-1498.

Kobayashi, S., Schultz, W., Sakagami, M., 2010. Operant conditioning of primate prefrontal neurons. J Neurophysiol 103, 1843-1855.

Lauwereyns, J., Sakagami, M., Tsutsui, K., Kobayashi, S., Koizumi, M., Hikosaka, O., 2001. Responses to task-irrelevant visual features by primate prefrontal neurons. J Neurophysiol 86, 2001-2010.

Leon, M.I., Shadlen, M.N., 1999. Effect of expected reward magnitude on the response of neurons in the dorsolateral prefrontal cortex of the macaque. Neuron 24, 415-425.

Liu, Y.H., Zhu, J., Constantinidis, C., Zhou, X., 2021. Emergence of prefrontal neuron maturation properties by training recurrent neural networks in cognitive tasks. iScience 24, 103178.

Mazrooyisebdani, M., Nair, V.A., Loh, P.L., Remsik, A.B., Young, B.M., Moreno, B.S., Dodd, K.C., Kang, T.J., William, J.C., Prabhakaran, V., 2018. Evaluation of Changes in the Motor Network Following BCI Therapy Based on Graph Theory Analysis. Front Neurosci 12, 861.

Miller, E.K., Cohen, J.D., 2001. An integrative theory of prefrontal cortex function. Annu Rev Neurosci 24, 167-202.

Mohanty, R., Sinha, A.M., Remsik, A.B., Dodd, K.C., Young, B.M., Jacobson, T., McMillan, M., Thoma, J., Advani, H., Nair, V.A., Kang, T.J., Caldera, K., Edwards, D.F., Williams, J.C., Prabhakaran, V., 2018. Machine Learning Classification to Identify the Stage of Brain-Computer Interface Therapy for Stroke Rehabilitation Using Functional Connectivity. Front Neurosci 12, 353.

Newton, A.T., Morgan, V.L., Rogers, B.P., Gore, J.C., 2011. Modulation of steady state functional connectivity in the default mode and working memory networks by cognitive load. Hum Brain Mapp 32, 1649-1659.

Papoutsi, M., Weiskopf, N., Langbehn, D., Reilmann, R., Rees, G., Tabrizi, S.J., 2018. Stimulating neural plasticity with real-time fMRI neurofeedback in Huntington's disease: A proof of concept study. Hum Brain Mapp 39, 1339-1353.

Parthasarathy, A., Herikstad, R., Bong, J.H., Medina, F.S., Libedinsky, C., Yen, S.C., 2017. Mixed selectivity morphs population codes in prefrontal cortex. Nat Neurosci 20, 1770-1779.

Pereira, D.J., Sayal, A., Pereira, J., Morais, S., Macedo, A., Direito, B., Castelo-Branco, M., 2023. Neurofeedback-dependent influence of the ventral striatum using a working memory paradigm targeting the dorsolateral prefrontal cortex. Front Behav Neurosci 17, 1014223.

Qi, X.L., Constantinidis, C., 2012a. Correlated discharges in the primate prefrontal cortex before and after working memory training. Eur J Neurosci 36, 3538-3548.

Qi, X.L., Constantinidis, C., 2012b. Variability of prefrontal neuronal discharges before and after training in a working memory task. PLoS One 7, e41053.

Qi, X.L., Meyer, T., Stanford, T.R., Constantinidis, C., 2011. Changes in prefrontal neuronal activity after learning to perform a spatial working memory task. Cereb Cortex 21, 2722-2732.

Qi, X.L., Meyer, T., Stanford, T.R., Constantinidis, C., 2012. Neural correlates of a decision variable before learning to perform a match/non-match task. J Neurosci 32, 6161-6169.

Rainer, G., Rao, S.C., Miller, E.K., 1999. Prospective coding for objects in primate prefrontal cortex. J Neurosci 19, 5493-5505.

Rouzitalab, A., Boulay, C.B., Park, J., Martinez-Trujillo, J.C., Sachs, A.J., 2023. Ensembles code for associative learning in the primate lateral prefrontal cortex. Cell Rep 42, 112449.

Sakagami, M., Niki, H., 1994. Encoding of behavioral significance of visual stimuli by primate prefrontal neurons: relation to relevant task conditions. Exp Brain Res 97, 423-436.

Sakai, K., Miyashita, Y., 1991. Neural organization for the long-term memory of paired associates. Nature 354, 152-155.

Sakurai, Y., 2001. Working memory for temporal and nontemporal events in monkeys. Learn Mem 8, 309-316.

Seitz, A.R., 2013. Cognitive neuroscience: targeting neuroplasticity with neural decoding and biofeedback. Curr Biol 23, R210-212.

Shibata, K., Watanabe, T., Sasaki, Y., Kawato, M., 2011. Perceptual learning incepted by decoded fMRI neurofeedback without stimulus presentation. Science 334, 1413-1415.

Spaak, E., Watanabe, K., Funahashi, S., Stokes, M.G., 2017. Stable and Dynamic Coding for Working Memory in Primate Prefrontal Cortex. J Neurosci 37, 6503-6516.

Wang, X.J., 2002. Probabilistic decision making by slow reverberation in cortical circuits. Neuron 36, 955-968.

Wang, X.J., 2008. Decision making in recurrent neuronal circuits. Neuron 60, 215-234.

Watanabe, K., Funahashi, S., 2014. Neural mechanisms of dual-task interference and cognitive capacity limitation in the prefrontal cortex. Nat Neurosci 17, 601-611.

Watanabe, K., Funahashi, S., 2018. Toward an understanding of the neural mechanisms underlying dual-task performance: Contribution of comparative approaches using animal models. Neurosci Biobehav Rev 84, 12-28.

Watanabe, M., Hikosaka, K., Sakagami, M., Shirakawa, S., 2007. Reward expectancy-related prefrontal neuronal activities: are they neural substrates of "affective" working memory? Cortex 43, 53-64.

Watanabe, M., Sakagami, M., 2007. Integration of cognitive and motivational context information in the primate prefrontal cortex. Cereb Cortex 17 Suppl 1, i101-109.

Widge, A.S., Boggess, M., Rockhill, A.P., Mullen, A., Sheopory, S., Loonis, R., Freeman, D.K., Miller, E.K., 2018. Altering alpha-frequency brain oscillations with rapid analog feedback-driven neurostimulation. PLoS One 13, e0207781.

Zhang, G., Yao, L., Shen, J., Yang, Y., Zhao, X., 2015. Reorganization of functional brain networks mediates the improvement of cognitive performance following real-time neurofeedback training of working memory. Hum Brain Mapp 36, 1705-1715.

Zhang, G., Yao, L., Zhang, H., Long, Z., Zhao, X., 2013. Improved Working Memory Performance through Self-Regulation of Dorsal Lateral Prefrontal Cortex Activation Using Real-Time fMRI. PLoS One 8, e73735.

Figure legends

Figure 1. Recording area and delayed matching-to-paired sample task (DMPST). **a**. Schematic cortical map of the recording site in the left lateral prefrontal cortex (*left*) and magnetic resonance image of monkey S (*right*). Neurons around the caudal part of the principal sulcus were recorded (shaded circle area). **b.** Task sequence of behavioral events. Gray area depicts the delay period. ITI, inter-trial interval **c.** Sample–test stimulus matching in the DMPST. **d.** Block sequence, delay-length modulation, and the controller of rectangle movement during the delay period.

Figure 2. Delayed matching-to-paired sample task performance with and without neurofeedback. **a.** Correct performance (monkey M, *left*; monkey S, *right*) in the control (white bars) and neurofeedback (gray bars) blocks. **b.** Shorter delay lengths in the neurofeedback blocks than in the control blocks ($p < 0.01$, Mann-Whitney *U*-test). Solid line depicts the median delay-length modulation in the neurofeedback blocks. Fine dashed line represents zero delay-length modulation, corresponding to the delay length in the control block. Dashed line depicts the fitted quadratic regression curve. **c.** Larger standard deviation in the neurofeedback blocks induced larger error rates. Solid and dashed lines indicate the significance of linear regression analysis (*ps* < 0.01, Pearson's correlation test) for stimuli A and B, respectively. **d.** Proportion of error types (fixation-break and choice errors) in the control and neurofeedback blocks. White stars denote significant differences ($p < 0.01$, paired *t*-test). White and gray bars indicate the control and feedback blocks, respectively. The same convention was used as in **a**. **e.** Choice-error rates as a function of delay-length modulation. The mean proportion of choice error was calculated in each bin (100 ms, no overlap) of the delay-length modulation. Data from both monkeys were merged. Error bars in **a** and **d** represent the standard error of the mean.

Figure 3. Activity of the modulated neuron types. **a.** Schematic activity of Type I (*upper*), II (*middle*), and III (*bottom*) neurons. Filled and open stars indicate the statistical significance of factor effects and their interaction, respectively. a.u. arbitrary units. **b–d.** Activity of Type I (**b**), II (**c**), and III (**d**) neurons. Representative (*upper*) and population (*bottom*) activities of each neuron type are displayed. Rastergrams and histograms of the representative neurons are aligned to the time of sample stimulus onset. Black and red tick marks depict spike timing in the control and neurofeedback blocks, respectively. Vertical dashed lines indicate the start of the delay period. Curves illustrate the mean firing rates of population activity (Type I: $n = 54$; Type II: $n = 15$; Type III: $n = 13$) for the different sample stimuli (Type I: stimulus A, thin curves; stimulus B, thick curves; Type II and III: non-preferred stimulus, thin curves; preferred stimulus, thick curves). Shaded areas with gradation represent variable delay duration. Note that the preferred and

non-preferred stimuli were determined dependent on the delay activity in the neurofeedback blocks. Colors represent the control (black) and neurofeedback (red) blocks.

Figure 4. Correct performance rates of each neuron type as a function of delay-length modulation in three epochs (**a**) and trial development of neuronal activity for each type (**b–d**). **a.** Correct performance was retained with moderate delay-length modulation (-600–0 ms) but not out of this range (< -600 ms) when the preferred stimulus of Type III neurons was tested under neurofeedback. Note that sample sizes depend on the delay-length modulation epochs and that the positions of neuron types do not indicate exact delay-length modulation. Stars indicate statistical significance (*ps* < 0.05, *t*-tests). **b–d**. Activity modulation of Type I (**b**), Type II (**c**), and Type III (**d**) neurons during the delay period in the first 15 trials in the neurofeedback blocks. For Type I neurons, black squares and white circles illustrate activity modulation for the stimuli in the neurofeedback block compared with the control block (**b**). For the other two types of neurons, lines display activity modulation for the preferred (red) and non-preferred (black) stimuli (**c** and **d**). Shaded areas with gradation in **d** represent variable delay duration. Error bars indicate the standard error of the mean. Black stars denote significant differences in firing rate between the stimuli during the delay in the trial (*t*-tests, *ps* < 0.05). A divergence of neuronal modulation during the delay period between the preferred vs. non-preferred stimuli developed throughout the trials.

Figure 5. Firing rate and numbers of irrelevant neuron types. Type I (*n* = 27, *left*), Type II (*n* = 6, *middle*), and Type III (*n* = 13, *right*) neurons. Irrelevant neurons were recorded simultaneously without neurofeedback of their neuronal activity. Error bars depict the standard error of the mean.

Figure 6. Behavior and neuronal activity in the yoked blocks compared with the control and neurofeedback blocks. **a.** The decreased correct performance rate in the neurofeedback blocks recovered in the yoked blocks to the same level as in the control blocks. **b.** Correct performance rate was not well fitted with a quadratic regression curve, but instead was well fitted with a linear regression line (dashed line). **c.** The same trial variance of the delay length used in the neurofeedback blocks did not correlate with the correct performance for either stimulus in the yoked blocks. **d.** Comparison of population activity of Type I–III neurons (Type I, *upper*; Type II, *middle*; Type III, *right*) among the three blocks (control and neurofeedback blocks: *n* = 54, yoked blocks: *n* = 37 for Type I; control and neurofeedback blocks: *n* = 15, yoked blocks: *n* = 10 for Type II; control and neurofeedback blocks: *n* = 15, yoked blocks: *n* = 4 for Type III). Black, red, and blue represent the control, neurofeedback, and yoked blocks, respectively. **e.** Mean activity at 500–1 ms before target option appearance of Type I–III neurons among the three blocks. The same colors were

assigned to depict the blocks as in **d**.

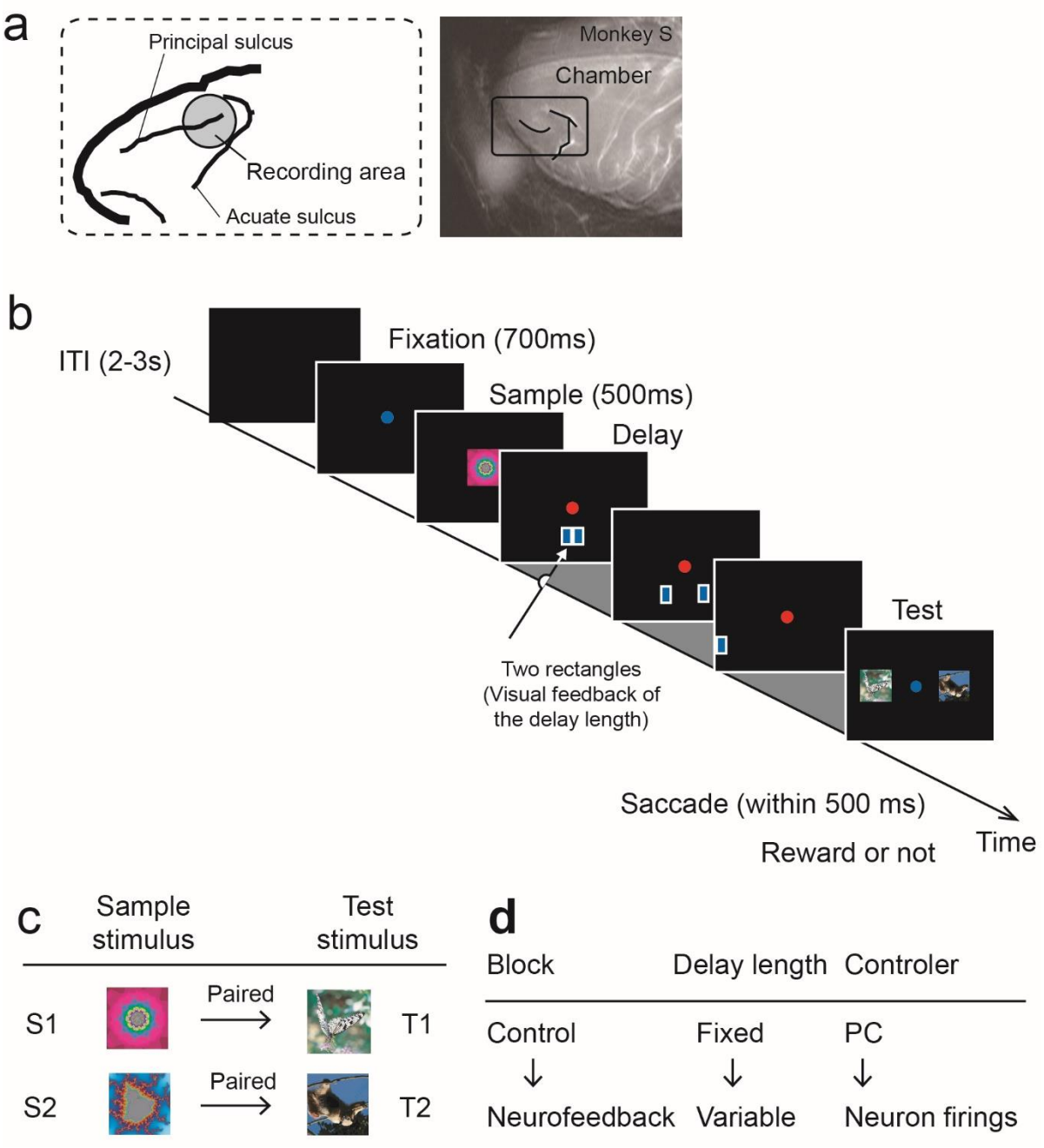
a
Principal sulcus
Recording area
Acuate sulcus
Monkey S
Chamber
b
ITI (2-3s)
Fixation (700ms)
Sample (500ms)
Delay
Test
Two rectangles
(Visual feedback of
the delay length)
Saccade (within 500 ms)
Reward or not
Time
c
Sample stimulus
Test stimulus
S1
Paired
T1
S2
Paired
T2
d
Block
Delay length
Controler
Control
Fixed
PC
Neurofeedback
Variable
Neuron firings

Figure 1

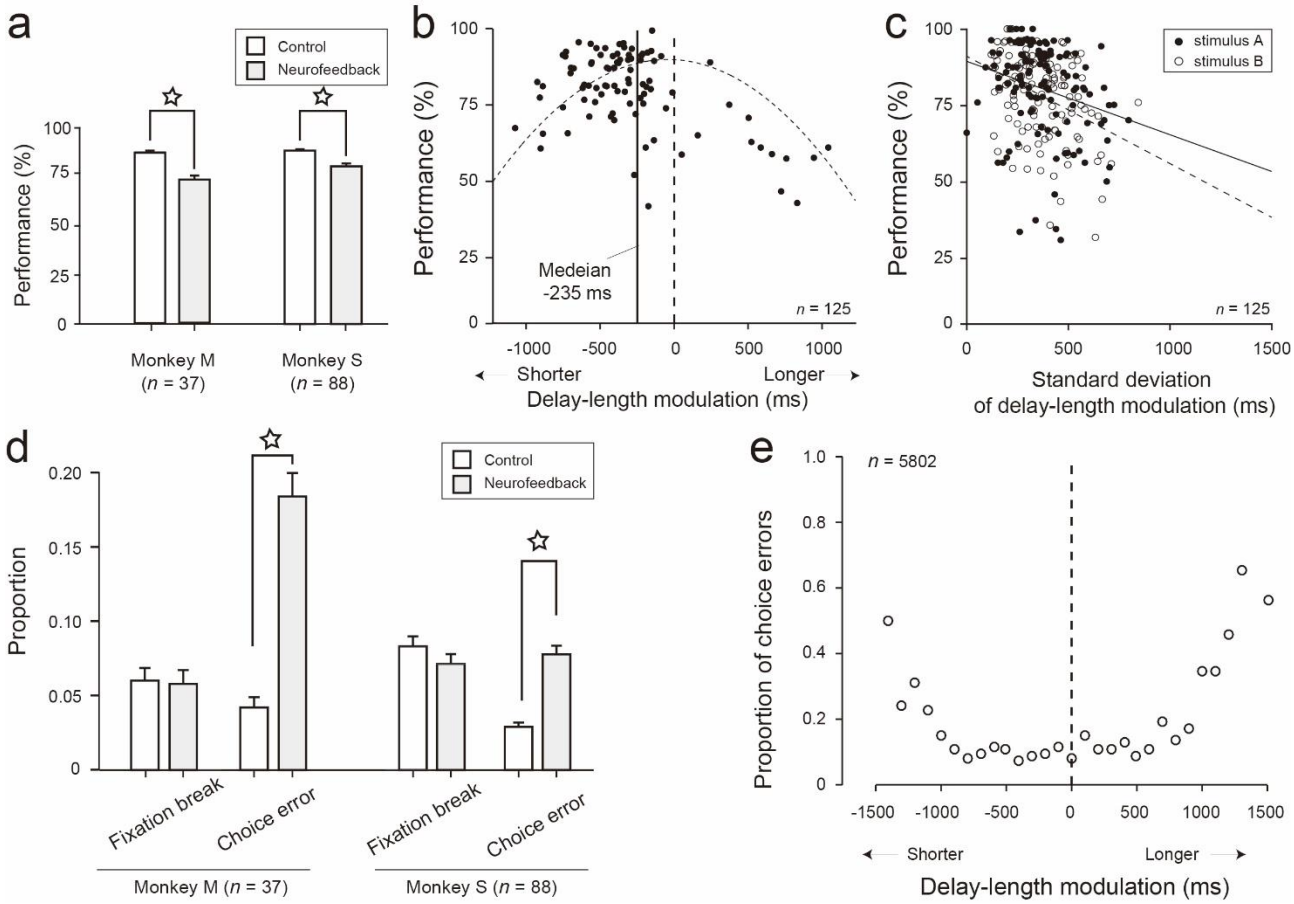
a
Control
Neurofeedback
Performance (%)
100
75
50
25
0
Monkey M
(n = 37)
Monkey S
(n = 88)
b
Performance (%)
Medeian
-235 ms
n = 125
-1000
-500
0
500
1000
Shorter
Longer
Delay-length modulation (ms)
c
stimulus A
stimulus B
Performance (%)
n = 125
0
500
1000
1500
Standard deviation
of delay-length modulation (ms)
d
Control
Neurofeedback
Proportion
0.20
0.15
0.10
0.05
0
Fixation break
Choice error
Fixation break
Choice error
Monkey M (n = 37)
Monkey S (n = 88)
e
n = 5802
Proportion of choice errors
1.0
0.8
0.6
0.4
0.2
0
-1500
-1000
-500
0
500
1000
1500
Shorter
Longer
Delay-length modulation (ms)

Figure 2

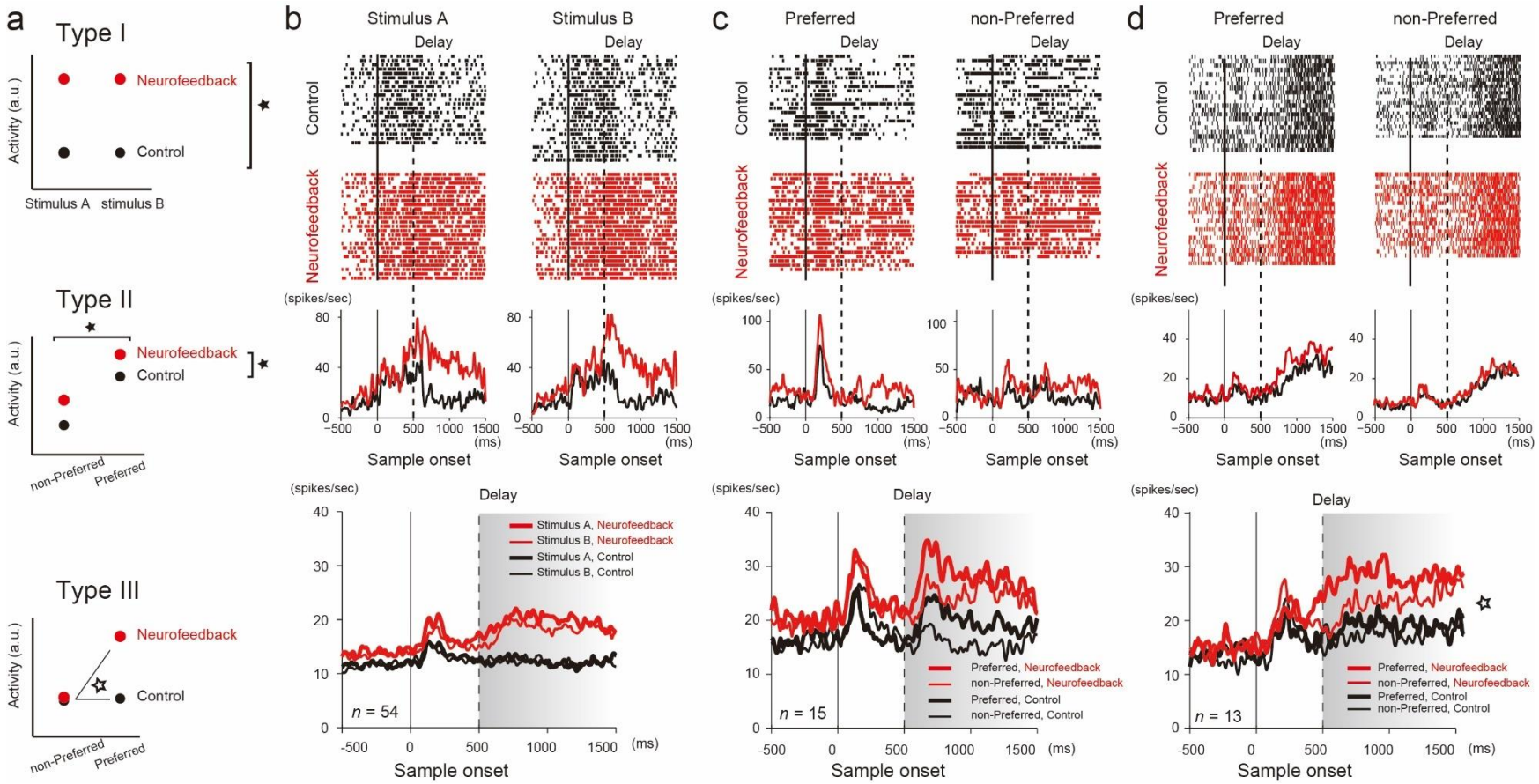
a
Type I
Activity (a.u.)
Neurofeedback
Control
Stimulus A
stimulus B
Type II
Activity (a.u.)
Neurofeedback
Control
non-Preferred
Preferred
Type III
Activity (a.u.)
Neurofeedback
Control
non-Preferred
Preferred
b
Stimulus A
Stimulus B
Delay
Control
Neurofeedback
(spikes/sec)
Sample onset
(ms)
Stimulus A, Neurofeedback
Stimulus B, Neurofeedback
Stimulus A, Control
Stimulus B, Control
n = 54
c
Preferred
non-Preferred
Preferred, Neurofeedback
non-Preferred, Neurofeedback
Preferred, Control
non-Preferred, Control
n = 15
d
Preferred
non-Preferred
Preferred, Neurofeedback
non-Preferred, Neurofeedback
Preferred, Control
non-Preferred, Control
n = 13

647

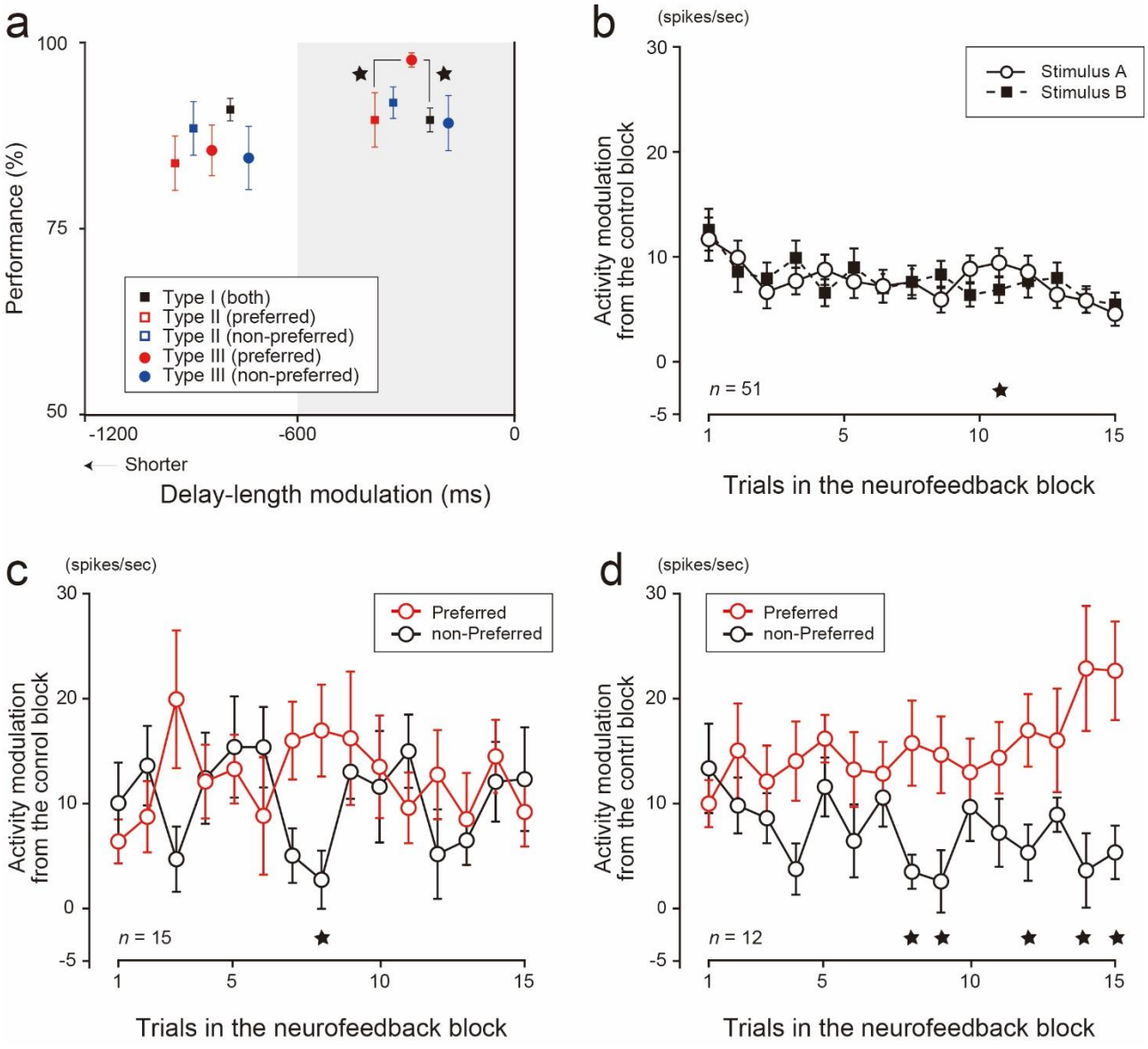
a
Performance (%)
100
75
50
-1200
-600
0
Shorter
Delay-length modulation (ms)
Type I (both)
Type II (preferred)
Type II (non-preferred)
Type III (preferred)
Type III (non-preferred)
b
(spikes/sec)
Activity modulation from the control block
Stimulus A
Stimulus B
n = 51
Trials in the neurofeedback block
c
(spikes/sec)
Activity modulation from the conrol block
Preferred
non-Preferred
n = 15
Trials in the neurofeedback block
d
(spikes/sec)
Activity modulation from the contrl block
Preferred
non-Preferred
n = 12
Trials in the neurofeedback block

Figure 4

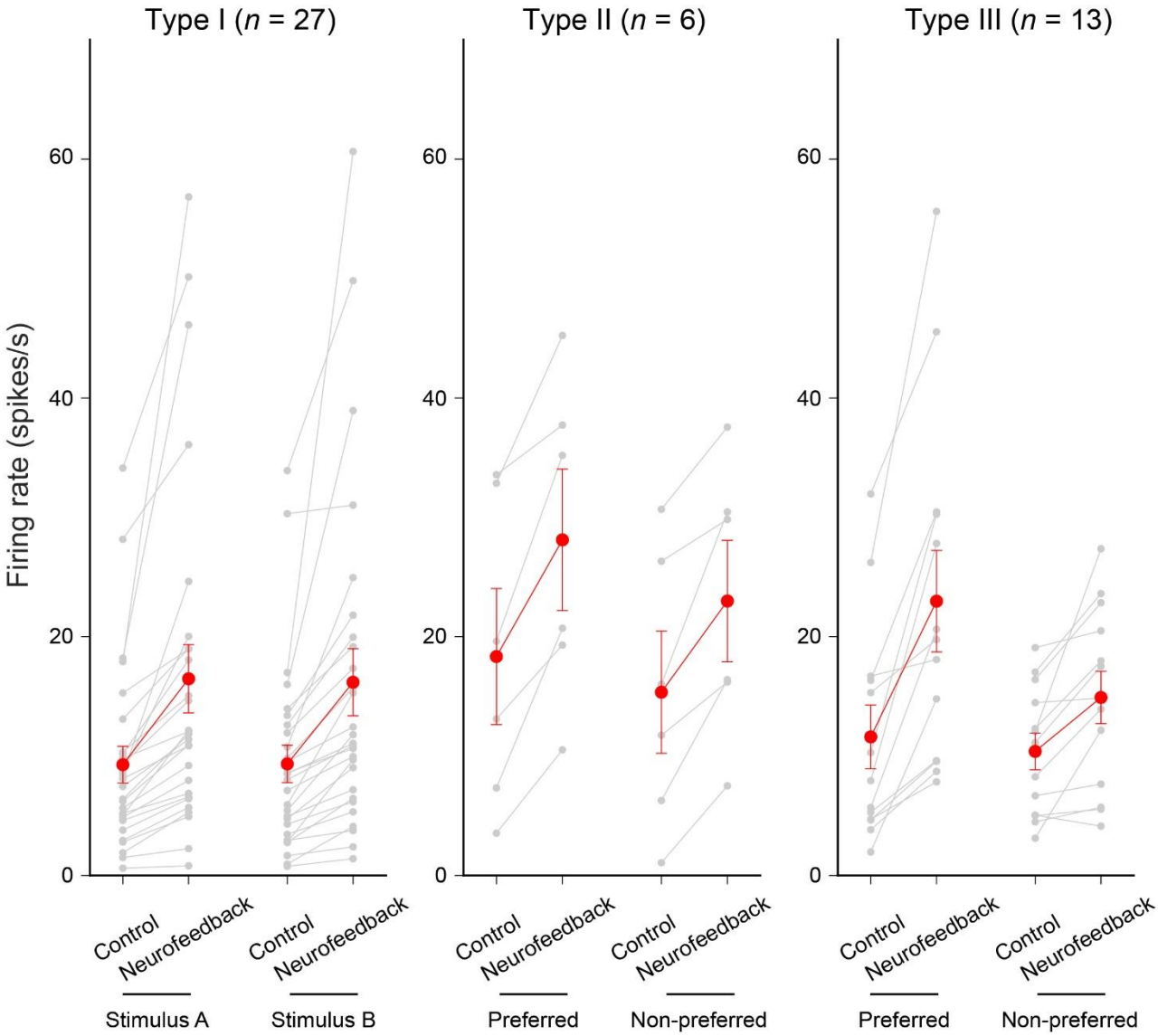
Type I (n = 27)
Type II (n = 6)
Type III (n = 13)
Firing rate (spikes/s)
0
20
40
60
Control
Neurofeedback
Stimulus A
Stimulus B
Preferred
Non-preferred

Figure 5

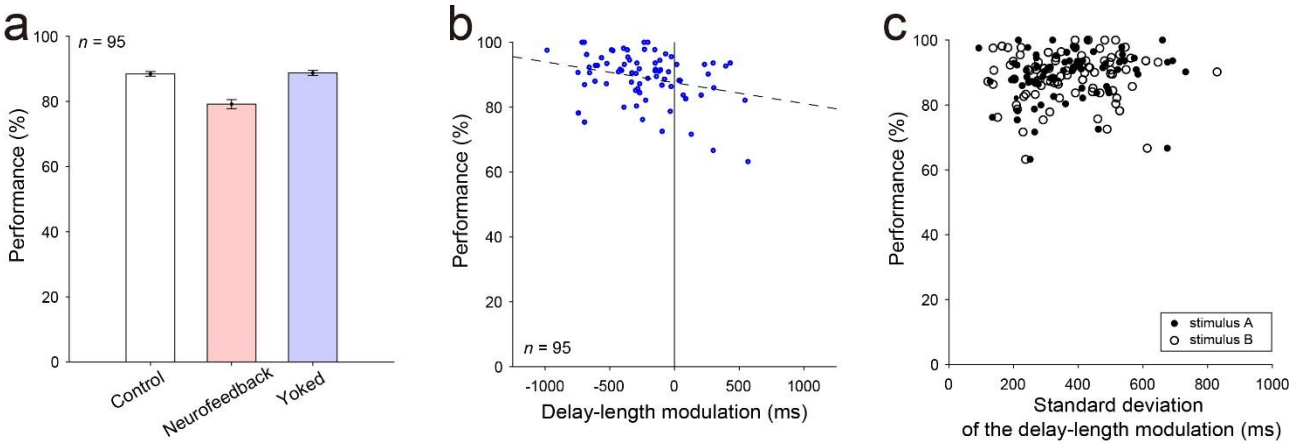
a
n = 95
Performance (%)
Control
Neurofeedback
Yoked
b
n = 95
Performance (%)
Delay-length modulation (ms)
c
Performance (%)
stimulus A
stimulus B
Standard deviation
of the delay-length modulation (ms)

Figure 6

Supplementary

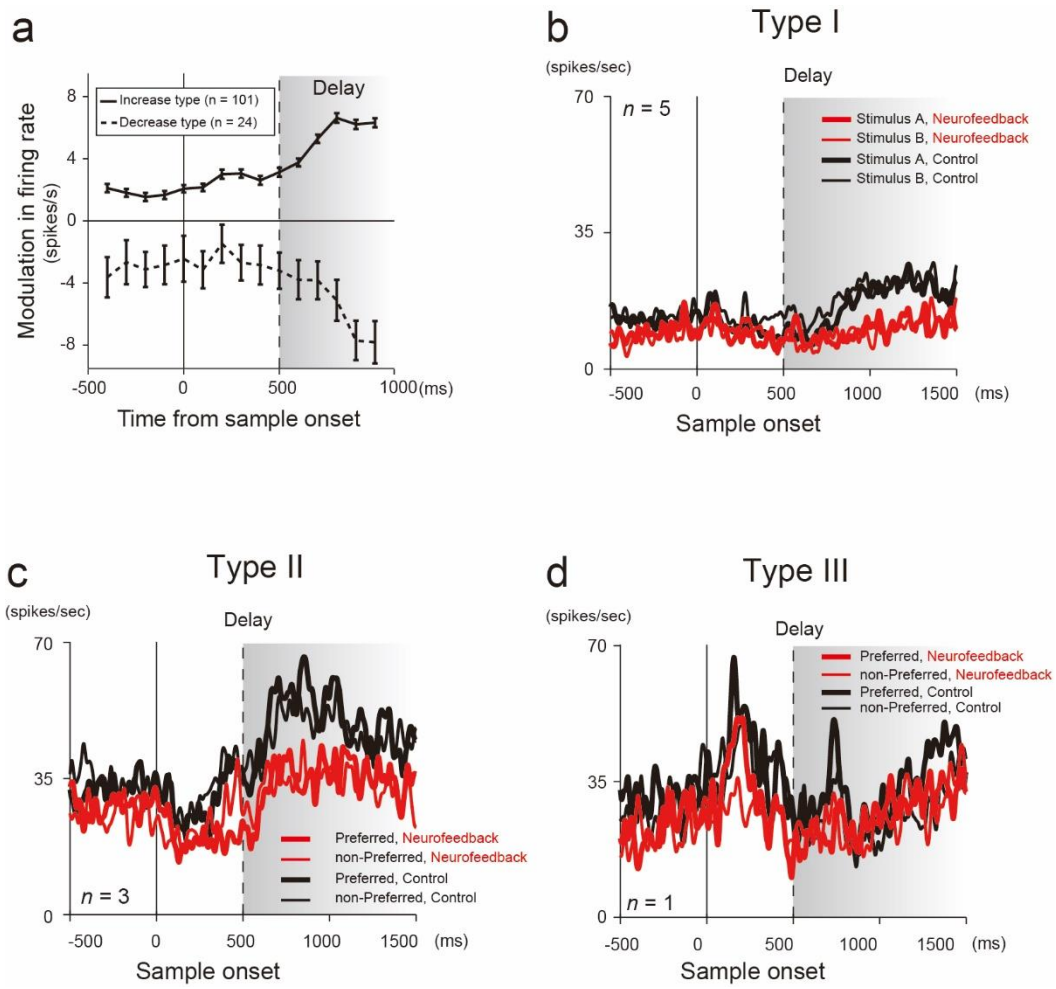

Figure S1

Figure S1. Decrease type activity. **a.** Comparison of delay activity between the increase and decrease neuronal types based on simple mean activity. The modulated activity after fixation onset between these neuron types was significantly different ($p < 0.05$, *t*-test was applied independently); the increased type exhibited significantly higher excitatory activity after fixation onset than during the inter-trial interval (spontaneous activity), whereas the decreased type showed inhibitory activity. **b–d.** Activity of decreased Type I (**b**), II (**c**), and III (**d**) neurons. Vertical dashed lines indicate the start of the delay period. Curves illustrate the mean firing rates of population activity (Type I: $n = 5$; Type II: $n = 3$; Type III: $n = 1$) of the sample stimuli (Type I: stimulus A, thin curves; stimulus B, thick curves; Type II and III: non-preferred stimulus, thin curves; preferred stimulus, thick curves). Shaded areas with gradation represent variable delay duration. Note that the preferred and non-preferred stimuli were determined dependent on the delay activity

in the neurofeedback blocks. Colors represent the control (black) and neurofeedback (red) blocks. The same convention was used as in Figure 3.